Bull. Mater. Sci. (2022) 45:199
https://doi.org/10.1007/s12034-022-02787-1

Ln^{3+} (Eu^{3+} and Dy^{3+}) luminescence in $Ca_2SrAl_2O_6$ phosphor for solid-state lighting

A N YERPUDE[1,*], S K RAMTEKE[1], V B PAWADE[2], N S KOKODE[3] and S J DHOBLE[4]
[1]Department of Physics, N.H. College, Brahmapuri 441206, India
[2]Department of Applied-Physics, LIT, RTM Nagpur University, Nagpur 440033, India
[3]N.H. College, Brahmapuri 441206, India
[4]Department of Physics, RTM Nagpur University, Nagpur 440033, India
*Author for correspondence (atulyerpude@gmail.com)

MS received 20 April 2022; accepted 17 June 2022

Abstract. This article reports photoluminescence in Eu^{3+} and Dy^{3+} doped $Ca_2SrAl_2O_6$ aluminate phosphor. Here combustion technique is used to synthesize a series of phosphors. The excitation spectra of $Ca_2SrAl_2O_6$:Eu^{3+} phosphor appears at 396 nm, under which we get a prominent emission bands at 590–596 nm and another peak located at 616 nm that corresponds to the orange-red region. These spectral bands are assigned due to $^5D_0 \rightarrow {}^7F_1$, $^7F_2$ electronic transitions of activator Eu^{3+} ion, respectively. Whereas, $Ca_2SrAl_2O_6$:Dy^{3+} phosphor shows two bands that correspond to 476 and 573 nm when excited by 352 nm. These two emission peaks correspond to the well-known $^4F_{9/2} \rightarrow {}^6H_{15/2}$, $^6H_{13/2}$ transitions of rare-earth Dy^{3+} ion, respectively. Thus, from the observed photoluminescence properties, it is seen that prepared aluminate phosphor may be a suitable material for solid-state lighting.

Keywords. Photoluminescence; lanthanides; synthesis; SSL.

1. Introduction

At present, white light-emitting diodes gain more importance in smart display technology as well as received more considerable interest due to their energy saving capabilities and environmental sustainability as compared to traditional incandescent and fluorescent lamp [1–4]. In the literature specifically two approaches have been discussed for the production of pure white in LEDs device. For which we can use either multicomponent or single component phosphor for fabrication of white light-emitting diode. The first approach has been developed with the combination of UV-LED chip coupled with red, green and blue phosphors for producing white light. Therefore, it required an efficient RGB-emitting phosphor that is activted by well-known impurites like Eu, Mn, Dy and Ce in appropriate host lattices [5–11]. While for a single-phase phosphor, white light can be generated through the energy transfer from sensitizers to activators, such as Ce–Eu, Eu–Mn, Ce–Mn, etc. [10–16]. In red-emitting phosphors, the ion Eu^{3+} is commonly utilized as an activator, where an emission is mainly due to $^5D_0 \rightarrow {}^7F_J$ (J = 0, 1, 2, 3, 4) electronic transition of Eu^{3+} ion under near-UV excitation and is highly dependent upon local site symmetry of the Eu^{3+} ion in host lattice [17–20]. The inversion centre around Eu^{3+} ions plays an important role on the emission intensity. A strong and narrow red emission peak at $\sim$620 nm is observed by doping Eu^{3+} ion into lattice sites of lower symmetry [21]. Amongst the various hosts, aluminate is one of the most important host in producing phosphor for LED applications because of its unique optical properties, chemical and physical stability as well as reproducibility. YAG:Ce is commercially used in producing white LED's in combination with blue chip of InGaN [22]. An aluminate nitride phosphor $CaAlSiN_3$:Eu^{2+} is also commercially in use as red-emitting phosphor for the fabrication of multicomponent white LED [23]. The solid-state method and combustion methods are generally in use for the synthesis of aluminate phosphors, which are having their own advantages as a low cost and less time-consuming reaction methods. In this paper, our aim is to develop a multi-colour emitting lanthanide-doped phosphor for application in solid-state lighting, which has been synthesized by well-known combustion technique.

2. Experimental

A series of Eu^{3+} doped $Ca_2SrAl_2O_6$ aluminate phosphor has been prepared by combustion technique. Initially, stoichiometric amount of the metal nitrates and urea were calculated and used as reactants. For the preparation of $Ca_2SrAl_2O_6$:Eu^{3+} phosphor, raw materials used are $Ca(NO_3)_2$, $Sr(NO_3)_2$, $Al(NO_3)_3$, $(NH_2)_2CO$ and Eu_2O_3. The

Published online: 13 October 2022

Eu_2O_3 was converted into nitrate form by adding appropriate amount of HNO_3 to it. All the weighed quantities of each nitrates and urea (all AR grade) are added and the mixture is crushed together in a mortar for 1/2 h to form a thick paste. The resulting paste is placed in a silica crucible and held at 550°C in a muffle furnace. The mixture undergoes highly exothermic reaction and bursts into flame, which persists for ∼30 s resulting in a white foamy product. The crucible is then taken out of the furnace, cooled and the foamy product was crushed to obtain fine power. This powdered sample is then used for characterization. Similar process was used for preparation of $Ca_2SrAl_2O_6$:Dy^{3+}. The photoluminescence measurement was carried out using Shimadzu RF5301PC Spectrofluorophotometer. At room temperature, this Spectrofluorophotometer gives corrected excitation and emission spectra in the 220–400 and 300–700 nm ranges, respectively. For each measurement, 2 g samples were used. A spectral slit width of 1.5 nm was used to record the excitation and emission spectra.

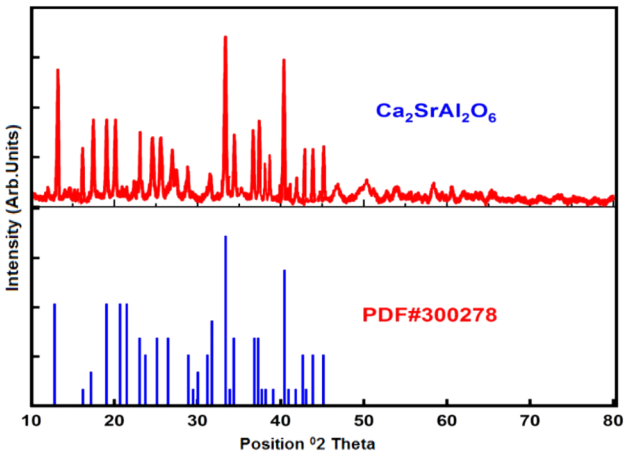

Figure 1. XRD of host $Ca_2SrAl_2O_6$ phosphor.

3. Result and discussion

3.1 *X-ray diffraction*

Phase purity and crystallinity of the materials was checked by powder X-ray diffraction (XRD) pattern. Figure 1 shows the XRD patterns of $Ca_2SrAl_2O_6$ powder samples prepared by combustion method at 550°C. The analysis of XRD data of $Ca_2SrAl_2O_6$ phases is usually qualitative, just based on relative peak intensities. The XRD patterns of $Ca_2SrAl_2O_6$ powder samples were compared with those of the standard JCPDS No. 300278 and it was well matched.

3.2 *Scanning electron micrographs*

The surface shape and particle size of the $Ca_2SrAl_2O_6$ phosphor was investigated using scanning electron micrograph. Figure 2 shows the representative scanning electron micrographs taken at different magnifications. It can be seen from the scanning electron micrograph image that samples take on irregular in shape and the particle size was distributed between 5 and 10 µm.

3.3 *$Ca_2SrAl_2O_6$:Eu^{3+} phosphor*

The powdered samples of $Ca_2SrAl_2O_6$:Eu^{3+} were characterized for photoluminescence emission and excitation over

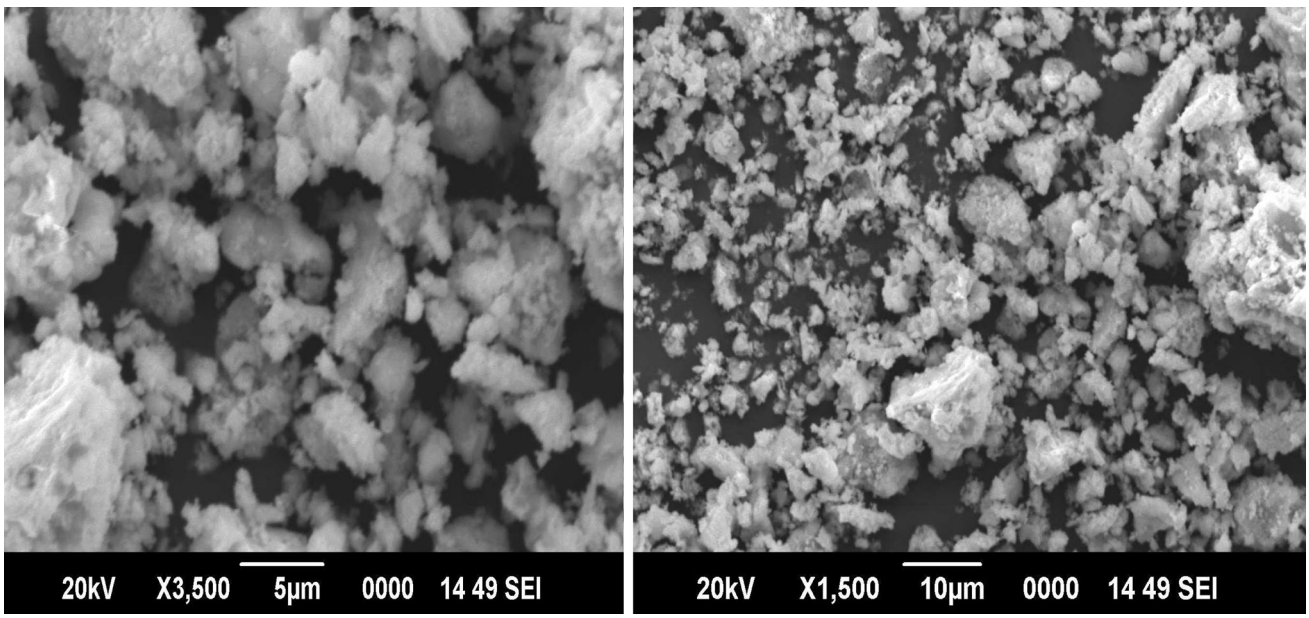

Figure 2. Scanning electron micrograph images of $Ca_2SrAl_2O_6$ phosphor.

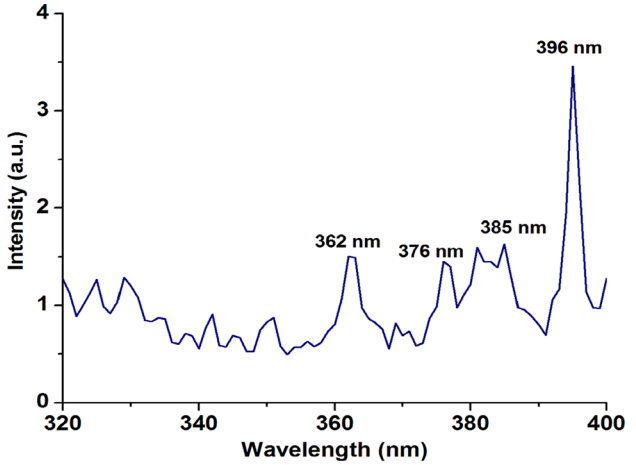

Figure 3. Photoluminescence excitation spectrum of $Ca_2SrAl_2O_6:Eu^{3+}$phosphor.

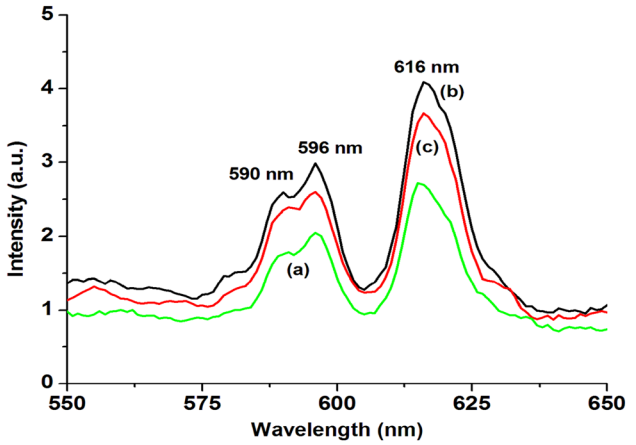

Figure 4. Photoluminescence emission spectra of $Ca_2SrAl_2O_6$:-Eu^{3+} phosphor: (a) 0.3, (b) 0.5 and (c) 1.0 mol%.

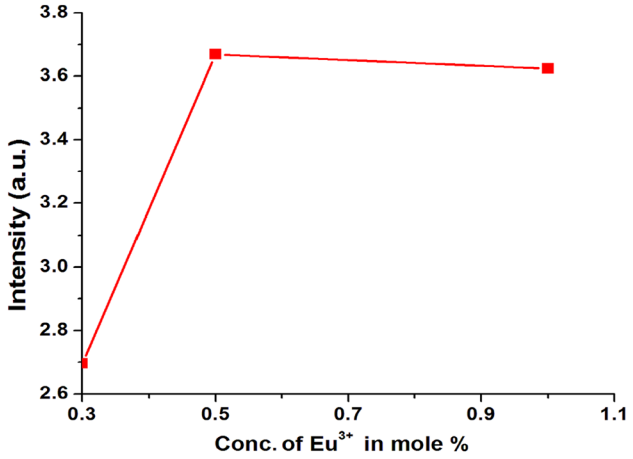

Figure 5. Effect of concentration of doped Eu^{3+} on relative luminescent intensity at 616 nm for $Ca_2SrAl_2O_6:Eu^{3+}$ phosphor.

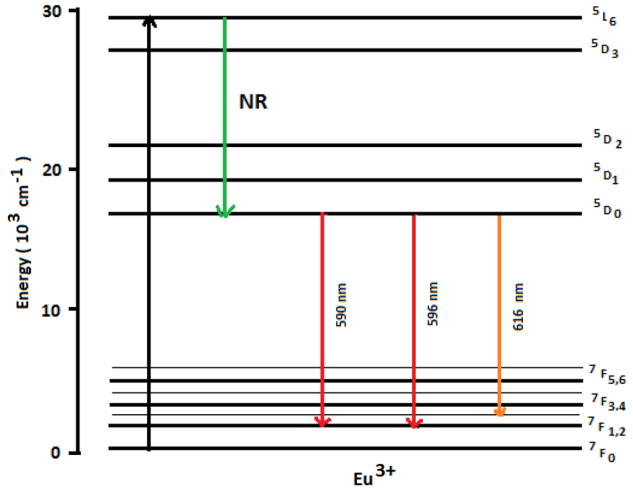

Figure 6. Energy transition diagram of Eu^{3+} ion.

the UV and visible region of electromagnetic spectrum. Figure 3 shows the excitation spectra of as-prepared $Ca_2SrAl_2O_6:Eu^{3+}$ phosphor. A prominent peak at 396 nm wavelength is clearly observed, which is characteristic of the dopant Eu^{3+}. This excitation wavelength is used to obtain the emission spectra, as shown in figure 4. A doublet at 590–596 nm and another peak at 616 nm in the orange-red region were observed in the emission spectra. These emission wavelengths are assigned to $^5D_0 \rightarrow {}^7F_1$, $^7F_2$ electronic transitions of activator Eu^{3+} ion [24–27]. Whereas, the presence of doublet is an indication of the crystal field effect possibly due to perturbation during doping process. Figure 5 shows the effect of Eu^{3+} concentration on emission intensity. From figure 5 it clearly indicates that as we increase the concentration of europium ions from 0.3 to 0.5 mol%, the emission intensity increases after that emission intensity decrease due to concentration quenching effect. The highest emission intensity is located at 0.5 mol%. Energy transition diagram of Eu^{3+} ion is shown in figure 6. The photoluminescence properties clearly suggest that with optimization in photoluminescence characteristics the prepared aluminate phosphor may be used for applications in solid-state lighting, especially white light-emitting diodes).

3.4 *$Ca_2SrAl_2O_6:Dy^{3+}$ phosphor*

The excitation spectra of $Ca_2SrAl_2O_6:Dy^{3+}$ phosphor is shown in figure 7. The multiple peaks correspond to UV region of the electromagnetic spectrum at 328, 352, 367 and 390 nm corresponding to f→f transitions of rare-earth Dy^{3+} ion. Amongst them, the 352 nm peak has the highest intensity corresponding to $^6H_{15/2} \rightarrow {}^4F_{9/2}$ excitation transition of Dy^{3+} ion and is used to monitor the photoluminescence emission spectra of the phosphor [28,29]. The emission spectra of $Ca_2SrAl_2O_6:Dy^{3+}$ for different concentrations of the activator corresponding to excitation wavelength 352 nm is shown in figure 8. The emission spectra show two bands, one located at 476 nm, i.e., in the

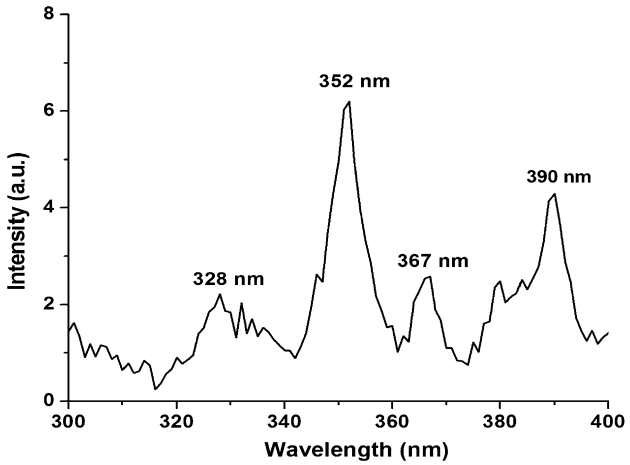

Figure 7. Excitation spectrum of $Ca_2SrAl_2O_6:Dy^{3+}$ phosphor.

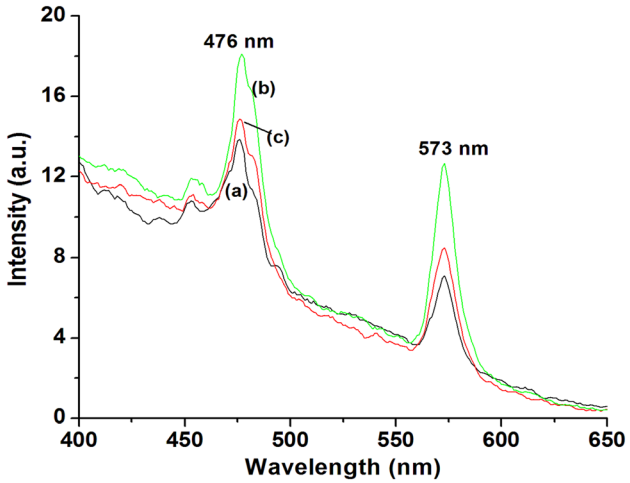

Figure 8. Emission spectra of $Ca_2SrAl_2O_6:Dy^{3+}$ phosphor, where λ_{ex}=352 nm: (a) Dy^{3+}=0.2 mol%, (b) Dy^{3+}=0.5 mol% and (c) Dy^{3+}=1 mol%.

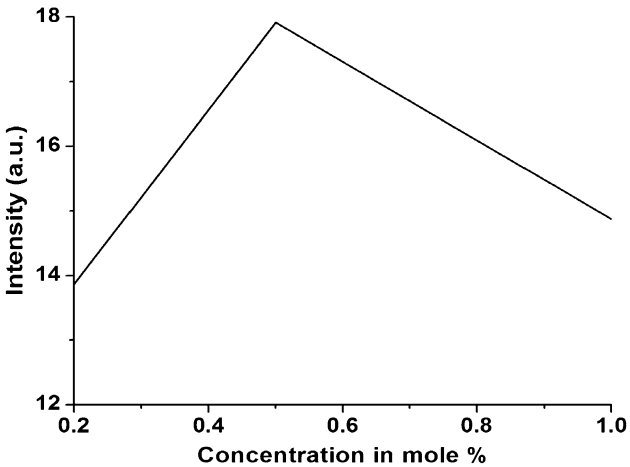

Figure 9. Effect of concentration of doped Dy^{3+} on relative luminescent intensity at 476 nm for $Ca_2SrAl_2O_6:Dy^{3+}$ phosphor.

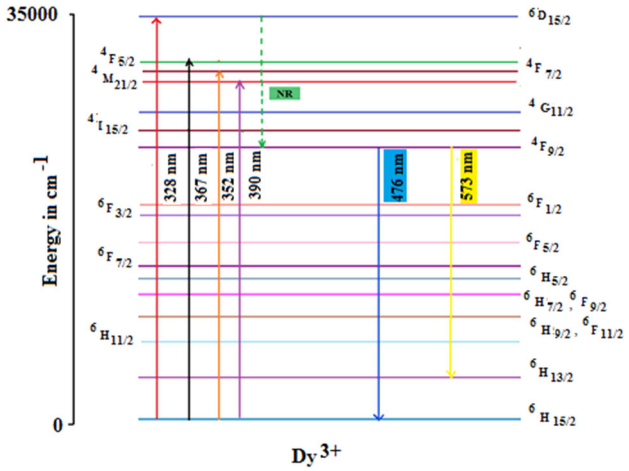

Figure 10. Energy transition diagram of Dy^{3+} ion.

blue region and other at 573 nm in the yellow region. These two emission peaks corresponds to the well-known $^4F_{9/2}\rightarrow{}^6H_{15/2}$, $^6H_{13/2}$ transitions of rare-earth Dy^{3+} ion. As shown in figure 9, as the concentration of the activator is increased from 0.2 mol% initially the intensity increases at 0.5 mol% but then emission intensity decreases as the concentration is increased to 1 mol%. The decrease in intensity of emission is ascribed to concentration quenching effect [25]. This change occurs due to resonant energy transition between Dy^{3+}-Dy^{3+} ions and its different cross-relaxation. The resonant energy transition takes place between $^4F_{9/2}\rightarrow{}^6H_{15/2}$ energy levels of Dy^{3+} ions [30]. The energy transition bands of Dy^{3+} ion depicted at $^6H_{15/2}\rightarrow{}^6D_{15/2}$ (328 nm), $^6H_{15/2}\rightarrow{}^4F_{7/2}$ (352 nm), $^6H_{15/2}\rightarrow{}^4F_{5/2}$ (367 nm) and $^6H_{15/2}\rightarrow{}^4M_{21/2}$ (390 nm), due to 4f-4f transitions. The significant excitation transition $^6H_{15/2}\rightarrow{}^4F_{7/2}$ at 352 nm was chosen among all the transitions for recording the emission spectra of Dy^{3+} activated $Ca_2SrAl_2O_6$. The photoluminescence spectra consists of two characteristics emission bands ascribed to transitions at $^4F_{9/2}\rightarrow{}^6H_{15/2}$ (476 nm: yellow), $^4F_{9/2}\rightarrow{}^6H_{15/2}$ (573 nm: blue), as shown in figure 10 [31–33].

4. Conclusion

Eu^{3+} and Dy^{3+} activated $Ca_2SrAl_2O_6$ phosphor was synthesized by combustion technique and it was well characterized by photoluminescence measurement. $Ca_2SrAl_2O_6:Eu^{3+}$ gives a prominent peak at 396 nm and emission spectra gives doublet at 590, 596 nm and another peak at 616 nm in the orange-red region corresponding to $^5D_0\rightarrow{}^7F_1$, $^7F_2$ electronic transitions of activator Eu^{3+} ion incorporated in the aluminate host. The strongest excitation peak of $Ca_2SrAl_2O_6:Dy^{3+}$ phosphor was observed at 352 nm. The emission spectra corresponding to excitation wavelength 352 nm shows two peaks, one at 478 nm wavelength in the blue region corresponds to transition

$^4F_{9/2} \rightarrow {}^6H_{15/2}$ and other at 573 nm wavelength in the yellow region corresponds to transition $^4F_{9/2} \rightarrow {}^6H_{13/2}$. The photoluminescence properties clearly suggest that prepared phosphor could be applicable in solid-state lighting technology.

Acknowledgements

A N Yerpude is thankful to Gondwana University, Gadchiroli, India (Project Ref. No. No./GUG/DIIL/609/2020, dated 14/02/2020) for financial assistance and constant encouragement.

References

[1] Li X, Budai J D, Liu F, Howe J Y, Zhang J, Wang X J *et al* 2013 *Light: Sci. Appl.* **2** 50
[2] Ramteke S K, Yerpude A N, Kokode N S, Shinde V V and Dhoble S J 2020 *J. Mater. Sci.: Mater. Electron.* **31** 6506
[3] Lin C C and Liu R S 2011 *J. Phys. Chem. Lett.* **2** 1268
[4] Park J K, Lim M A, Kim C H, Park H D, Park J T and Choi S Y 2003 *Appl. Phys. Lett.* **85** 683
[5] Schlotter P, Schmidt R and Schneider J 1997 *J. Appl. Phys. A* **64** 417
[6] Yerpude A N, Nikhare G N, Dhoble S J and Kokode N S 2019 *Mater. Today: Proc.* **15** 511
[7] Tsai Y T, Chiang C Y, Zhou W, Lee J F, Sheu H S and Liu R S 2015 *J. Am. Chem. Soc.* **137** 8936
[8] Lian H, Huang Q, Chen Y, Li K, Liang S, Shang M *et al* 2017 *Inorg. Chem.* **56** 11900
[9] Yerpude A N and Dhoble S J 2016 *Optik* **127** 4217
[10] Pushpendra Singh S, Srinidhi S, Kunchala R K, Kalia R, Achary S N *et al* 2021 *Cryst. Growth Design* **21** 4619
[11] Shah A Y, Wadawale A, Naidu B S, Vatsa R K, Jain V K, Dhayal V *et al* 2010 *Inorg. Chim. Acta* **363** 3680
[12] Guo C, Luan L, Xu Y, Gao F and Liang L 2008 *J. Electrochem. Soc.* **155** J310
[13] Ding W, Wang J, Liu Z, Zhang M, Su Q and Tang J 2008 *J. Electrochem. Soc.* **155** J122
[14] Liu Y, Zhang X, Hao Z, Wang X and Zhang J 2011 *Chem. Commun.* **47** 10677
[15] Pushpendra, Kunchala R K, Achary S N and Naidu B S 2019 *ACS Appl. Nano Mater.* **2** 5527
[16] Pushpendra, Kunchala R K, Achary S N, Tyagi A K and Naidu B S 2019 *Cryst. Growth Design* **19** 3379
[17] Kasturi S and Sivakumar V 2017 *Mater. Chem. Front.* **1** 550
[18] Serra O A, Cicillini S A and Ishiki R R 2000 *J. Alloys Compd.* **303** 316
[19] Gaft M, Reisfeld R, Panczer G, Shoval S, Champagnon B and Boulon G 1997 *J. Lumin.* **72** 572
[20] Pushpendra, Suryawanshi I, Kalia R, Kunchala R K, Mudavath S L and Naidu B S 2022 *J. Rare Earths* **40** 572
[21] Neeraj S, Kijima N and Cheetham A K 2004 *Chem. Phys. Lett.* **387** 2
[22] Pust P, Schmidt P J and Schnick W 2015 *Nat. Mater.* **14** 454
[23] Piao X, Machida K, Horikawa T, Hanzawa H, Shimomura Y and Kijima N 2007 *Chem. Mater.* **19** 4592
[24] Ramteke S K, Kokode N S, Yerpude A N, Nikhare G N and Dhoble S J 2020 *Luminescence* **35** 618
[25] Yerpude A N, Dhoble S J and Kokode N S 2019 *Optik* **179** 774
[26] Panse V R, Yerpude A N, Dhoble S J, Kokode N S and Choithrani R 2017 *J. Mater. Sci.: Mater. Electron* **28** 16880
[27] Yerpude A N, Panse V R, Dhoble S J, Kokode N S and Srinivas M 2017 *Luminescence* **32** 1361
[28] Dhoble S J, Kore B P, Yerpude A N, Kohale R L, Yawalkar P W and Dhoble N S 2015 *Optik* **126** 1527
[29] Baig N, Dhoble N S, Yerpude A N, Singh V and Dhoble S J 2016 *Optik* **127** 6574
[30] Linganna K, Rao C S and Jayasankar C K 2013 *J. Quant. Spectrosc. Radiat. Transfer* **118** 40
[31] Yerpude A N and Dhoble S J 2012 *J. Lumin.* **132** 1781
[32] Yerpude A N and Dhoble S J 2013 *Optik* **124** 3567
[33] Ramteke S K, Yerpude A N, Kokode N S and Dhoble S J 2021 *Bull. Mater. Sci.* **44** 174